Strojniški vestnik - Journal of Mechanical Engineering 70(2024)5-6, 247-258
DOI:10.5545/sv-jme.2023.787
Original Scientific Paper
Received for review: 2023-09-07
Received revised form: 2024-02-11
Accepted for publication: 2024-04-03

Effect of Laser Parameters on Surface Texture of Polyformaldehyde and Parameter Optimization

Fengren Li[1,2] – Chao Li[1,2,*] – Juan Zhou[3] – Jiantao He[1,2] – Jiebin Wang[1,2] – Cong Luo[1,2] – Si Li[1]

[1] Hunan Institute of Science and Technology, College of Mechanical Engineering, China
[2] Key Laboratory of Intelligent Manufacturing and Service Performance Optimization of Laser and Grinding in Mechanical Industry, China
[3] Yueyang Vocational Technical College, College of Electromechanical Engineering, China

This research aimed to investigate the influence of laser process parameters on the surface texture of Polyformaldehyde (POM) and to improve its processability and process predictability. A comparative experiment and analysis involving multiple processing parameters, including laser power, scanning speed, and pulse width, were conducted on POM. Statistical prediction models of laser processing POM were established among the laser power, scanning speed, pulse width, texture depth, surface roughness at the bottom of texture, and multi-objective optimization and experimental verification of process parameters were carried out based on the grey-Taguchi analysis method. Experimental results show that the laser power and scanning speed significantly affect the texture depth. Higher laser power and lower scanning speed are conducive to forming depth. The surface roughness at the bottom of the texture increases with the increase in scanning speed and shows a tendency to rise and then fall as the laser power increases. The surface roughness and texture depth obtained under the optimal process parameters($A_5B_1C_1$) are 1.373 μm and 466.891 μm, respectively, which were reduced by 10.08 % and increased by 3.42 % compared with the minimum surface roughness and maximum depth in the orthogonal experiments. The validation experiments of the prediction model show that it can meet the reliability requirements, and the errors of the predicted values of depth and surface roughness are 1.86 % and 7.60 %, respectively. The above research provides theoretical and experimental support for the precise control of surface texture prepared by laser processing POM.

Keywords: picosecond laser processing, parameter optimization, polyformaldehyde (POM), grey-Taguchi analysis method, prediction model

Highlights

- *The effect of laser parameters on the surface texture features of POM was studied.*
- *Established prediction models between laser parameters and texture features.*
- *The optimal parameter combination is obtained based on the grey-Taguchi method.*
- *Laser power and scanning speed have a significant effect on texture quality.*

0 INTRODUCTION

With the development of synthesis and processing technology for polymer materials, the use and scale of various polymers are growing rapidly [1] and [2]. As one of the most commonly used polymers today, POM has become a suitable substitute for traditional materials in many application fields (gears, seals, bearings, etc. [3]) due to its high stiffness, hardness, elastic modulus, excellent wear resistance, and low weight [4] to [6]. With the development of technology and industry, relying solely on the performance of the material itself has gradually failed to meet the requirements of surface performance. The method of enhancing surface performance by processing micro-texture on the material surface has been widely studied and applied [7] to [10]. Many techniques for fabricating surface structures have been developed, such as etching technologies [11], atomic layer deposition [12], abrasive jet processing [13], and micro-casting [14]. However, these methods are generally costly, and it is difficult to prepare micro-nanostructures on the material surface, which do not meet the current low-carbon processing concept and high-precision processing requirements.

In recent years, lasers have proven to be a powerful tool for the precise processing of structures at the micron and nanoscale. The unique feature of laser processing is that it can modify materials in multiple length dimensions and produce complex micro- and nanostructures [15] to [17], resulting in better surface properties. Most of the existing research focuses on laser processing of metals [18] and [19] and ceramics [20] and [21], with less emphasis on polymers [22]. The majority of research aims to improve surface performance by altering texture types while studying the geometric quality of the texture itself, and the effect of laser process parameters on the texture quality has become a hot topic in recent years. Zhao et al. [23] systematically investigated the effect of repetition frequency on hole size morphology and described the relationship between repetition

*Corr. Author's Address: College of Mechanical Engineering, Hunan Institute of Science and Technology, Yueyang 414006, China, lch@hnist.edu.cn

frequency and micropore size (such as diameter and depth) during picosecond laser ablation of metallic materials. Deepu et al. [24] investigated the effect of laser fluence, pulse overlap and pulse repetition rate on hole diameter, depth, and other factors. It was found that the best hole geometry could be obtained with a fluence of 0.44 J/cm, 10 kHz repetition rate and 85 % pulse overlap.

At present, the lack of research on process parameters is the key reason for the inability to consistently obtain surface textures with excellent structure and significant functionality. The interaction and coupling between various process parameters also make it difficult to establish a feasible and complete theoretical model. Therefore, to achieve precise control of laser processing and obtain better quality texture, it is crucial to establish a predictive model between process parameters and texture geometric features, as well as to optimize the process parameters. Some scholars have studied the relationship between the geometric characteristics of material surface texture and laser process parameters using various analytical methods. Lian et al. [25] established a predictive model for the relationship between laser process parameters and the width of the clad layer, surface roughness, and dilution rate. They analysed the impact of process parameters on various response variables, and experimental results showed that the predictive model had good accuracy. Cui et al. [26] established regression prediction models between process parameters and coating width, coating height, coating depth, aspect ratio and dilution rate. The average error between the predicted values of each regression prediction model and the experimentally measured values is less than 10 %.

To improve the surface performance of POM materials, it is necessary to achieve precise control of the surface texture of POM. In this paper, the elliptical texture is processed on the surface of POM by picosecond laser, and the influence of process parameters (laser power, scanning speed, pulse width) on the texture characteristics (depth, surface roughness) is investigated, and the relationship between process parameters and texture characteristic morphology is determined. The effect of process parameters on texture characteristics and the interaction between the process parameters were analysed using the grey-Taguchi method, and the optimal combination of process parameters was obtained for the elliptical texture. Also, a prediction model of the geometric characteristics of the surface texture of POM was established, which provides an experimental and theoretical basis for further optimization of ultrafast laser processing of POM materials.

1 EXPERIMENTAL

1.1 Materials and Equipment

The experiment sample is M90-type POM (YUNTIANHUA CO., Ltd., Yunnan, China) with the specification of 25 mm × 25 mm × 10 mm (length×width×thickness). The samples were ultrasonically cleaned in anhydrous ethanol before and after laser processing, then naturally dried and placed on a two-dimensional moving table, which was computer-controlled for precise movement along x and y directions. The laser processing system used in this experiment is shown in Fig. 1a, where the laser is an infrared ultrashort pulse picosecond laser developed and produced by LinitiaLase, and the main technical parameters of the laser are shown in Table 1. The 3D measuring laser microscope (LEXT

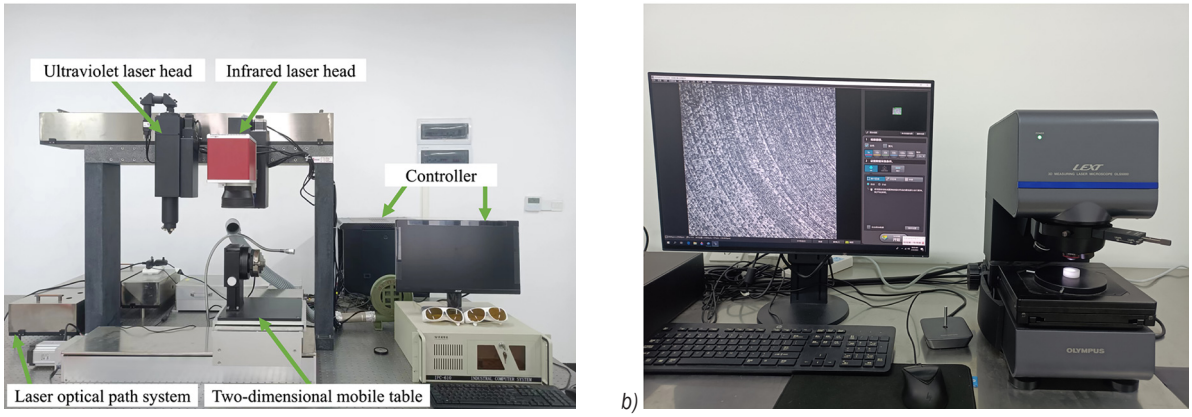

Fig. 1. *Experimental instruments; a) laser processing system, and b) 3D laser scanning microscope*

OLS5000, Olympus) shown in Fig. 1b enables fast and efficient accurate sub-micron 3D measurements and surface roughness measurements. It was used to observe the texture morphology and measure texture depth and surface roughness.

Table 1. *Main technical parameters of ultraviolet nanosecond laser*

Parameter	Value
Central wavelength [nm]	1028±5
Maximum output power [W]	30
Maximum pulse energy [μJ]	200
Laser frequency [kHz]	1 to 200
Pulse width [μs]	0.05 to 50
Beam divergence [urad]	<20
Beam quality [-]	M2<1.2

1.2 Experimental Design

1.2.1 Univariate Experiments

To study the effect of laser parameters on the geometry of the POM ellipse (long axis 1.5 mm × short axis 1 mm) texture, the controlled variable method was used to explore the effect of laser power, scanning speed and pulse width on the depth of texture and surface roughness. Table 2 displays the specific experimental parameters used, while Table 3 outlines the laser parameters that were not discussed in this study. During the laser processing, the POM workpiece is placed on a high-precision motion platform, and the pulse laser with high repetition frequency and high energy density is applied to the surface of the workpiece using different laser processing parameters [26], which is radiated on the surface of the specimen according to the set scanning path and causes it to melt and vaporize [27], thus processing the elliptical texture with a certain depth. The ultrasonic cleaning device was used to clean the processed samples. After natural air drying, the elliptical texture was observed and calculated with a 3D measuring laser microscope on the surface of the POM. To ensure the accuracy of the surface roughness measurement on the bottom surface of the texture, the overall measurement of the centre area of the elliptical texture bottom surface was performed using a 20× magnification, as shown in

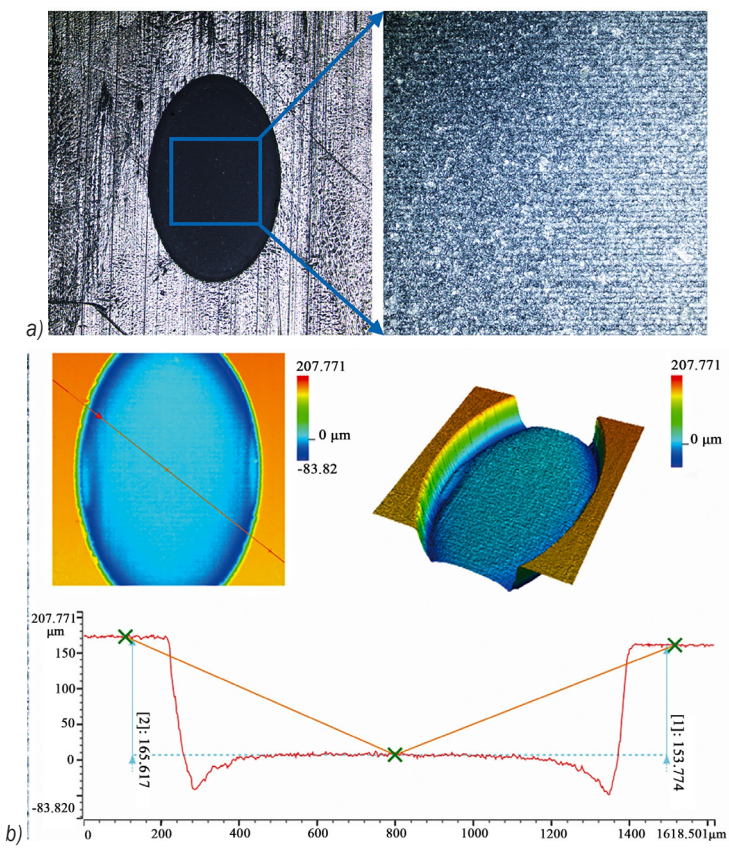

Fig. 2. *Measurement of a) surface roughness and b) depth*

Fig. 2a. The depth is measured as shown in Fig. 2b. Both values are taken as the average value after three repeated measurements.

Table 2. *Laser processing experimental parameters*

Laser power [W]	Scanning speed [mm·s^{-1}]	Pulse width [μs]
19.5, 21, 22.5, 24, 25.5, 27, 28.5, 30	600	12
24	450, 500, 550, 600, 650, 700, 750, 800	12
24	600	4, 12, 20, 28, 36, 44
24	600	12

Table 3. *Values of laser parameters not discussed*

Frequency [kHz]	Current strength [A]	Number of scans [-]	Laser line spacing [mm]	Ring spacing [mm]
60	1	10	0.005	0.5

1.2.2 Orthogonal Experimental Design

The Taguchi method is a local optimization algorithm based on an orthogonal experiment and signal-to-noise ratio (S/N) designed by Genichi Taguchi **[28]**. Orthogonal table design experiments can reasonably reduce the number of experiments and blindness. Statistical analysis of the experimental results with the S/N as a measure of quality characteristics can lead to the best combination of reliable and stable process parameters, achieving a combination of high efficiency and low cost. This article takes the depth of texture and surface roughness as the response targets, and the three process parameters of laser power, scanning speed, and pulse width are the influencing factors. The levels of the three process parameters are shown in Table 4. Based on the Taguchi experiment principle, the L_{25} (5^3) orthogonal experiment table with five levels and three factors is designed as shown in Table 5, where A, B, and C represent laser power, scanning speed, and pulse width, respectively. After the corresponding data were measured experimentally, the influencing factors of each response target were explored independently, and then the multi-mass target optimization problem was transformed into a single-objective optimization problem using grey correlation analysis to obtain the degree of influence **[29]**, trend, and the best process parameter combination of the three process parameters on the response target. The optimal process parameters were also used for laser processing to verify the effectiveness of process parameter optimization, and the accuracy of the model was verified by substituting it into the established prediction model for the solution. The measured data from the orthogonal experiments are shown in Table 6.

Table 4. *Factors and their levels*

Level	Factor		
	A Laser power [W]	B Scanning speed [mm·s^{-1}]	C Pulse width [μs]
1	18	400	4
2	21	500	12
3	24	600	20
4	27	700	28
5	30	800	36

Table 5. *L_{25} (5^3) Taguchi orthogonal experimental design*

No	A	B	C	No	A	B	C
1	18	400	4	14	24	700	4
2	18	500	12	15	24	800	12
3	18	600	20	16	27	400	28
4	18	700	28	17	27	500	36
5	18	800	36	18	27	600	4
6	21	400	12	19	27	700	12
7	21	500	20	20	27	800	20
8	21	600	28	21	30	400	36
9	21	700	36	22	30	500	4
10	21	800	4	23	30	600	12
11	24	400	20	24	30	700	20
12	24	500	28	25	30	800	28
13	24	600	36				

Table 6. *Results of orthogonal experiment*

No	Depth [μm]	Surface roughness [μm]	No	Depth [μm]	Surface roughness [μm]
1	197.142	1.558	14	227.206	3.268
2	171.335	1.527	15	204.575	4.099
3	148.198	1.883	16	394.915	2.429
4	134.415	2.190	17	338.945	2.259
5	118.957	2.559	18	299.383	2.504
6	289.134	1.947	19	267.142	3.812
7	251.768	2.149	20	241.586	4.371
8	216.943	2.618	21	451.443	3.289
9	190.783	3.273	22	394.611	1.942
10	166.790	3.701	23	340.797	3.151
11	354.549	2.237	24	300.774	4.819
12	296.081	2.098	25	267.183	5.598
13	260.960	2.601			

2 RESULTS AND DISCUSSION

2.1 Texture Morphology Analysis

2.1.1 Influence of Laser Power on Texture

To investigate the effect of laser power on the geometry of the texture, the surface of the POM sample was irradiated with lasers at power levels within the range of 19.5 W to 30 W under constant scanning speeds of 600 mm/s and pulse widths of 12 μs. The variation of the relevant parameters is shown in Fig. 3. With the gradual increase in laser power, the depth of elliptical texture shows an increasing trend, increasing from 160.709 μm to 302.197 μm. The increase in laser power means that the energy of individual laser pulses gradually increases, the energy density acting on the surface of POM increases, and when the laser energy density is higher than the ablation threshold of POM, the absorption of laser energy by POM produces ionization. The process of ionization becomes significant with increasing laser power, resulting in an increase in the volume of material removed and a greater depth of texture. Laser radiation to the site, with the increase in depth, began to move away from the original focal surface, and the laser energy to reach the bottom of the texture gradually decreased. Coupled with the gradual increase in the depth of the texture, the formation of molten spatter takes longer to fly out of the texture, as well as the laser processing process generated by the plasma on the laser shielding effect. As a result, the depth of the texture will increase with the laser power and tend to level off.

Meanwhile, it can be seen from Fig. 3 that the surface roughness of the elliptical texture bottom increases with the increase in laser power, but when the power reaches 24 W, the surface roughness reaches the maximum and continues to increase the power afterwards, the surface roughness starts to decrease instead. As shown in Fig. 4, the structure of the bottom surface of the texture structure is relatively regular when the laser power is small (19.5 W to 24 W), and most of the bottom surface is formed by the uniform cooling of the melt that fails to vaporize in time. However, as the laser power gradually increases, the melt vaporized on each laser path increases, and the melt that did not vaporize at this time could not effectively lap to form a good surface, thus making the overall surface roughness gradually increase. Also, when the laser power is higher (25.5 W to 30 W), the macrostructure of the texture bottom surface is poorer, but its overall surface roughness starts to decrease compared to the power of 24 W. This phenomenon is caused as follows: the melt vaporized on the laser sweeping path is more than the non-vaporized melt, and the non-vaporized melt becomes a single individual after cooling, thus forming a structure of multiple crystalline particles on a smooth surface on the bottom surface, at which time the overall surface roughness of the bottom surface will gradually decrease as the smooth surface area increases and the number and volume of crystalline particles decrease.

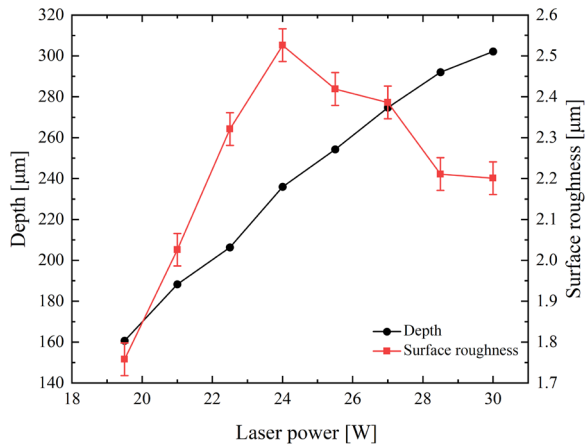

Fig. 3. *The changes in texture depth and surface roughness under different laser power*

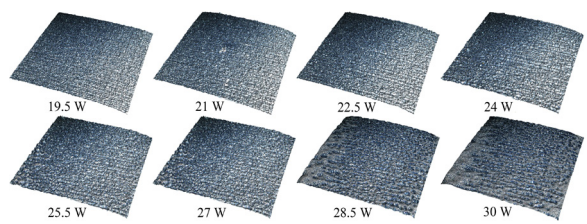

Fig. 4. *Texture bottom morphology under different laser power*

2.1.2 Influence of Scanning Speed on Texture

To further investigate the influence of laser scanning speed on texture, in a fixed other parameter situation, different laser scanning speeds (ranging from 450 mm/s to 800 mm/s with an increment of 50 mm/s) were employed for texture processing. The variations in texture-related parameters are shown in Fig. 5. From Fig. 5, it can be seen that the depth decreases with the increase in scanning speed, with a relatively stable depth variation within the range of 600 mm/s to 650 mm/s. The scanning speed affects the action time of the laser and the material surface. With the increase of the scanning speed, the laser irradiation time per unit area becomes shorter, and the number of times radiated by the pulsed laser becomes

less, the energy absorbed by the material surface decreases, and the material removal rate decreases, resulting in a decrease in the depth of the elliptical texture. Additionally, Fig. 5 indicates that the surface roughness of the bottom surface of the elliptical texture increases with increasing scanning speed, and the increase is gradually increasing. Combined with Fig. 6, it is found that the molten structure formed by laser ablation of POM gradually decreases with increasing scanning speed, and although the decrease of melt-like structure is beneficial to the macroscopic morphology, it has a negative effect on the surface roughness. As a common polymer, the crystallization properties of POM materials are positively correlated with heat treatment time and temperature in a specific temperature range [30]. As the scanning speed increases, the time for the texture to be radiated by the laser becomes shorter, the conduction and diffusion processes of energy on the material are shortened, the heat treatment time is shorter, and the crystallinity of the bottom surface of the texture is poor, which leads to the rise of its overall surface roughness.

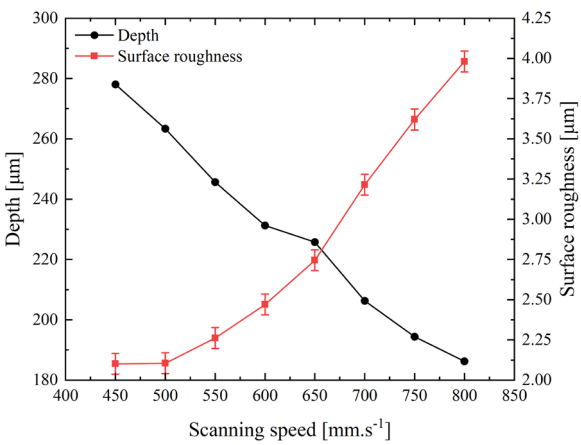

Fig. 5. *The changes in texture depth and surface roughness under different scanning speeds*

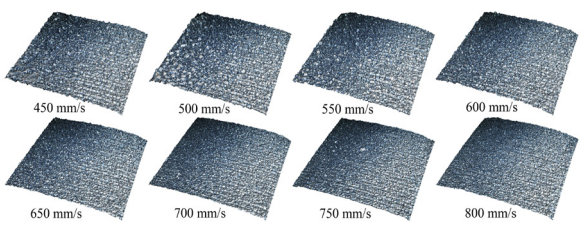

Fig. 6. *Texture bottom morphology under different scanning speed*

2.1.3 Influence of Pulse Width on Texture

Pulse width is an important parameter in laser processing, which represents the duration of laser pulse energy output. Under the condition of unchanged pulse energy, increasing the pulse width will extend the period during which each laser pulse acts on the material surface, consequently elevating the total heat absorbed by the material and expanding the thermally affected zone of the processing site. As can be seen from Fig. 7, the depth of the elliptical texture becomes more significant with increasing pulse width, and the depth of the texture increases from 215.591 μm to 224.512 μm when the pulse width increases from 4 μs to 44 μs, but the overall change is not significant. A comparison with Figs. 3 and 5 shows that the effect of pulse width on depth is much less than that of power and scanning speed. Fig. 7 also shows that the surface roughness of the texture's bottom surface fluctuates between 2.65 μm and 2.95 μm with the variation of pulse width, which is relatively small compared with the influences of power and scanning speed.

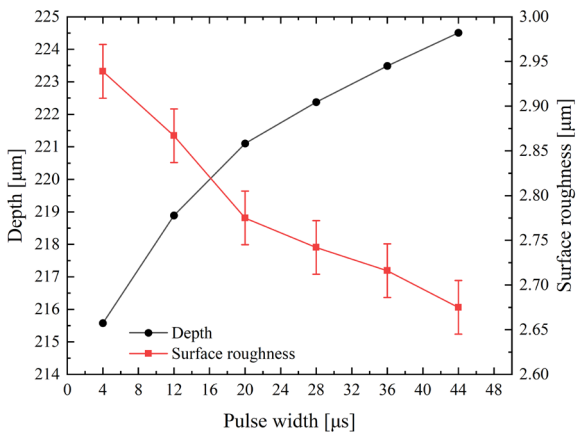

Fig. 7. *The changes of texture depth and surface roughness under different pulse width*

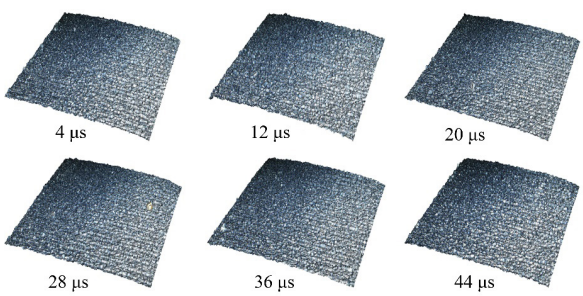

Fig. 8. *Texture bottom morphology under different pulse width*

During the process from a pulse width of 4 μs to 44 μs, the overall surface roughness exhibits a continuous decreasing trend. The rate of decrease is faster when the pulse width increases from 4 μs to 20 μs, while it becomes more moderate when the pulse width increases from 20 μs to 44 μs. From Fig. 8, it can

be observed that the morphology of the texture bottom surface does not undergo significant changes with increasing pulse width. Typically, larger pulse widths imply an extended duration of individual laser pulses and longer conduction times for laser energy inside the material, resulting in increased amounts of melt and corresponding changes in surface morphology. However, for a material like POM, variations in pulse width at the microsecond level have less effect on the melting process.

2.2 Model Building and Parameter Optimization

2.2.1 Model Building

Based on the data results obtained from the orthogonal experiment, the quadratic regression polynomials between laser power p, scanning speed v, pulse width w, depth D, and surface roughness Ra were constructed by Minitab. The obtained expressions are shown in Eqs. (1) and (2). According to the variance analysis results of depth shown in Table 7, the model coefficient P of the depth prediction model is much less than 0.05, indicating the high significance of the model at a 95 % confidence level. The multiple coefficients of determination R^2 value is 0.9957, and the adjusted R^2 value is 0.9945, both of which are close to 1, indicating the reliable predictive power of the model. Fig. 9a shows the residual normal plot of the depth regression model, from which it can be seen that the data points are evenly distributed around the fitted line with no abnormal data points, indicating a good fit for the regression model. In addition, the effect of pulse width on depth is not significant enough to exceed the 95 % confidence level, and variance analysis has automatically eliminated it. Similarly, as shown in Table 8 and Fig. 9b, the model coefficient P is less than 0.001, the P values of linear, square, and interaction terms are all less than 0.05, the multivariate coefficient R^2 is 0.9319, the adjusted R^2 is 0.9091, and the distribution of data points in the residual normal plot is reasonable, indicating that the prediction model has high overall reliability and fit.

2.2.2 Parameter Optimization

The Taguchi method evaluates the results of orthogonal experiments using the S/N ratio, which typically can be classified into three categories based on the research objectives: larger-the-better (LTB), smaller-the-better (STB), and nominal-the-best (NTB) [31]. In this study, the depth and surface roughness of the elliptical texture are chosen as the response variables. The objective was to achieve a large depth while maintaining a low surface roughness at a certain number of processing cycles. Therefore, the LTB criterion was used for the depth target, while the STB criterion was applied for the surface roughness target in calculating the S/N, and the magnitude of the influence of each process parameter on the target was sought using the range analysis. The specific results and data are shown in Tables 9 to 11, and the S/N ratio calculation formula is shown in Eq. (3).

$$D = -341.7 + 50.62p - 0.311v - 0.4673p^2 + 0.000381v^2 - 0.02036pv, \quad (1)$$

$$Ra = 8.74 - 0.0067p - 0.0247v + 0.0884w + 0.000015v^2 + 0.000572ps - 0.000119vw. \quad (2)$$

Table 7. *Variance analysis table of depth*

Source	Degree of freedom	Adj SS	Adj MS	F	P
Model	5	179199	35839.7	873.28	<0.001
Laser power (A)	1	5713	5713.3	139.21	<0.001
Scanning speed (B)	1	355	355.0	8.65	0.008
AA	1	1238	1238.3	30.17	<0.001
BB	1	1018	1017.8	24.80	<0.001
AB	1	3732	3732.3	90.94	<0.001
Pure Error	19	780	41.0		
Total	24	179978			
R^2 = 99.57 %			R^2(adj) = 99.45 %		

Table 8. *Variance analysis table of surface roughness*

Source	Degree of freedom	Adj SS	Adj MS	F	P
Model	6	24.4912	4.08186	41.03	<0.001
Laser power (A)	1	0.8477	0.84766	8.52	0.009
Scanning speed (B)	1	2.1672	2.16720	21.78	<0.001
Pulse width (C)	1	0.9156	0.91561	9.20	0.007
BB	1	1.6432	1.64322	16.52	0.001
AB	1	2.1639	2.16388	21.75	<0.001
BC	1	0.6701	0.67012	6.74	0.018
Pure Error	18	1.7909	0.09950		
Total	24	26.2821			
R^2 = 93.19 %			R^2(adj) = 90.91 %		

The degree of influence of each parameter on the texture depth at different levels can be seen in Tables 9 and 11. Due to the LTB characteristic of depth, when the combination of laser power (A), scanning speed (B), and pulse width (C) is set to $A_5B_1C_3$ (laser power

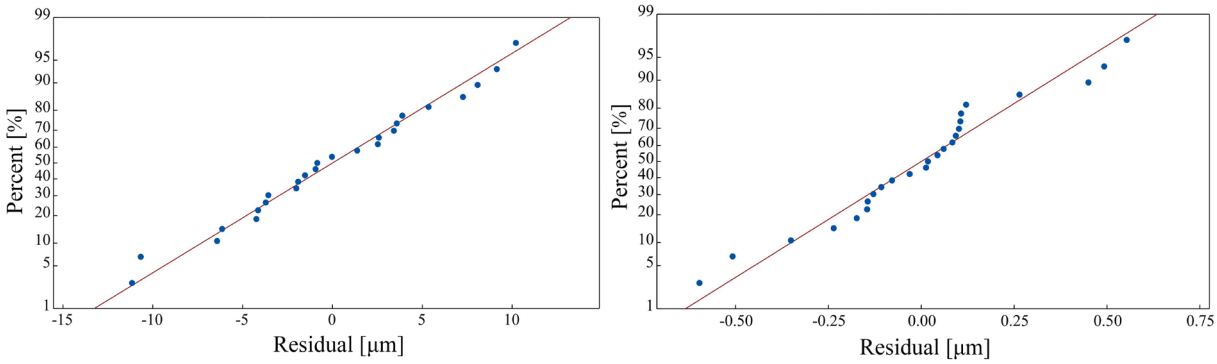

Fig. 9. *Normal probability plot of residuals for a) depth data and b) surface roughness data*

of 30 W, scanning speed of 400 mm/s, pulse width of 20 μs), this combination represents the optimal process parameter combination for controlling texture depth. Additionally, based on the extreme difference, the impact of each parameter on depth can be ranked in descending order as follows: laser power > scanning speed > pulse width. Similarly, the optimal combination of process parameters for controlling the surface roughness of the texture bottom surface is $A_1B_2C_1$ (laser power of 18 W, scanning speed of 500 mm/s, pulse width of 4 μs). The impact of each parameter on surface roughness can be ranked in descending order as follows: scanning speed > laser power > pulse width.

Although the optimal parameters of the two responses are obtained respectively, the optimal parameters of one response quantity could not take into account the other response quantity due to the different influence of each process parameter on both. To obtain the best combination of process parameters with two response quantities, the grey correlation method is used. The grey correlation method is a method to determine the significance of the relationship between factors in the order of grey correlation. The combination of grey relational analysis theory with the Taguchi method provides an effective solution for complex multi-response problems. By transforming multiple laser process parameter optimization problems into optimizing a single grey relational degree problem, the optimal combination of parameters can be obtained to achieve minimal surface roughness and maximum depth. The grey correlation analysis requires a series of calculations on the signal-to-noise data: S/N normalization, calculation of the grey correlation coefficient for each response quantity, and calculation of the grey correlation. The formulas used in the three steps are shown in Eqs. (4) to (6), and the final grey correlation values obtained by the three steps are shown in Table 12.

$$S/N=\begin{cases}-10\log\left(\dfrac{1}{n}\sum_{i=1}^{n}\dfrac{1}{y_i^2}\right) & LTB\\ -10\log\left(\dfrac{1}{n}\sum_{i=1}^{n}y_i^2\right) & STB\end{cases}, \tag{3}$$

where () is the value of the response quantity, is the number of experiments.

$$X_i(k)=\begin{cases}\dfrac{y_i(k)-\min y_i(k)}{\max y_i(k)-\min y_i(k)} & LTB\\ \dfrac{\max y_i(k)-y_i(k)}{\max y_i(k)-\min y_i(k)} & STB\end{cases}, \tag{4}$$

where $X_i(k)$ is the normalized value of the k^{th} response quantity for the i^{th} experiment; $y_i(k)$ is the value of the SNR for the i^{th} experiment of the k^{th} response quantity; $\max y_i(k)$ and $\min y_i(k)$ represent the maximum and minimum values of the k^{th} response volume in the 25 sets of experiments, respectively.

$$GRC_i(k)=\frac{\min_i\left|x_i^0-x_i(k)\right|+\xi\max_i\left|x_i^0-x_i(k)\right|}{\left|x_i^0-x_i(k)\right|+\xi\max_i\left|x_i^0-x_i(k)\right|}, \tag{5}$$

where $GRC_i(k)$ is the value of the grey correlation coefficient of the i^{th} experiment of the k^{th} response; $x_i(k)$ is the normalized value of the k^{th} response quantity for the i^{th} experiment; x_i^0 is the ideal value for the experiment, which is set to 1 in this study; ξ is the distinguishing coefficient which is defined in the range of $0\leq\xi\leq1$, ξ was taken as 0.5 in this study.

$$GRC_i=\frac{1}{n}\sum_{k=1}^{n}GRC_i(k), \tag{6}$$

where GRC_i is the grey correlation value of the i^{th} experiment; $GRC_i(k)$ is the value of the grey

correlation coefficient of the i^{th} experiment of the k^{th} response quantity; n is the number of response quantities and is 2 in this study.

Table 9. *SNR of response targets*

No.	Depth	Surface roughness	No.	Depth	Surface roughness
1	45.896	-3.851	14	47.128	-10.286
2	44.677	-3.677	15	46.217	-12.254
3	43.417	-5.497	16	51.930	-7.709
4	42.569	-6.809	17	50.603	-6.482
5	41.508	-8.161	18	49.525	-7.973
6	49.222	-5.787	19	48.535	-11.623
7	48.020	-6.645	20	47.661	-12.812
8	46.727	-8.359	21	53.092	-10.341
9	45.611	-10.299	22	51.923	-5.765
10	44.443	-11.366	23	50.650	-9.969
11	50.994	-6.993	24	49.565	-13.976
12	49.428	-6.436	25	48.536	-14.961
13	48.331	-8.303			

Table 10. *The SNR mean and range of depth*

Factor level	A	B	C
Mean 1	43.613	50.227	47.783
Mean 2	46.805	48.930	47.860
Mean 3	48.420	47.730	47.931
Mean 4	49.651	46.682	47.838
Mean 5	50.753	45.673	47.829
Range	7.140	4.554	0.148

Table 11. *The SNR mean and range of surface roughness*

Factor level	A	B	C
Mean 1	-5.599	-6.936	-7.848
Mean 2	-8.491	-5.801	-8.662
Mean 3	-8.854	-8.020	-9.185
Mean 4	-9.320	-10.599	-8.855
Mean 5	-11.002	-11.911	-8.717
Range	5.403	6.110	1.337

Table 12. *Grey relational analysis data*

No.	GRC	No.	GRC	No.	GRC
1	0.708	10	0.412	19	0.487
2	0.704	11	0.682	20	0.449
3	0.565	12	0.642	21	0.729
4	0.499	13	0.549	22	0.781
5	0.445	14	0.477	23	0.588
6	0.664	15	0.427	24	0.488
7	0.594	16	0.708	25	0.447
8	0.511	17	0.684		
9	0.448	18	0.593		

According to grey relational analysis theory, the degree of correlation between factors and the system depends on the value of the correlation degree. The larger the correlation deegree value of a process parameter, the greater its response in optimizing the objective function. Fig. 10 shows the main effect plot of the grey correlation of each process parameter, and it can be seen that the optimal process parameter is $A_5B_1C_1$, i.e., the laser power is 30 W, the scanning speed is 400 mm/s, and the pulse width is 4 μs.

2.2.3 Validation Analysis

Since the optimal combination of process parameters ($A_5B_1C_1$) was not included in the orthogonal experiment, a new set of machining experiments was conducted using the optimal parameter combination. Table 13 presents the optimized process parameters and the relevant parameters of the elliptical texture. Combining grey correlation theory with the data from the orthogonal experiment, the minimum surface roughness and maximum depth were selected as references. The surface roughness obtained from the optimized parameters was 1.373 μm, which decreased by 10.08 % compared to the minimum surface roughness obtained from the orthogonal experiment (1.527 μm); the depth obtained from the optimized parameters was 466.891 μm, which increased by 3.42 % compared to the maximum depth obtained from the orthogonal experiment (451.443 μm). The results demonstrate that the effect of the optimized parameters is consistent with the previous expectations, as it enables the simultaneous attainment of low surface roughness and a greater depth. It can also be seen from Fig. 11 that compared to the two texture substrates obtained through separate optimization using the Taguchi method, the substrate prepared after further optimization using the grey correlation method exhibits a greater abundance of molten-like structures.

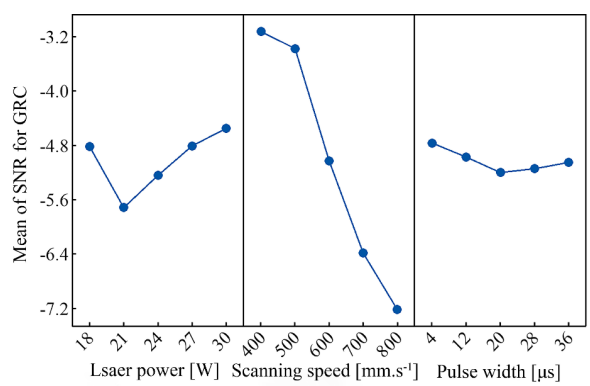

Fig. 10. *Main effects plot for the SNR analysis of GRC*

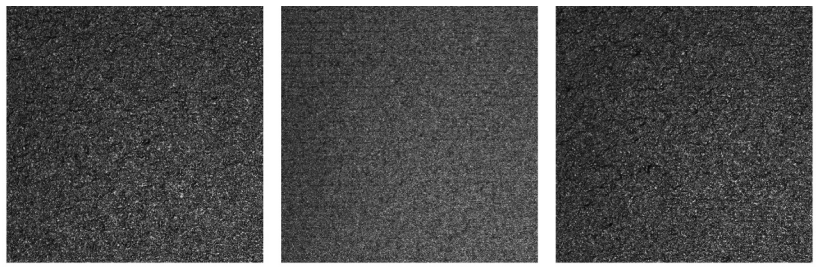

Fig. 11. *Texture bottom morphology under different parameter combinations*

Additionally, these molten structures are distributed in a wider and more uniform manner, which is also the reason for the further reduction in surface roughness. By substituting the optimal combination of process parameters into Eqs. (1) and (2), the predicted values for depth and surface roughness are obtained as 475.570 μm and 1.486 μm, respectively, and the errors between these predicted values and the actual measured values are 1.86 % and 7.60 %. This shows that the predictive model exhibits high accuracy and reliability, meeting the objectives of predicting and optimizing process parameters, and it has a positive effect on the accurate control of the texture morphology and quality as well as the improvement of the efficiency of ablation.

Table 13. *Optimized parameters and response*

Laser power [W]	Scanning speed [mm·s^{-1}]	Pulse width [μs]	Depth [μm]	Surface roughness
30	400	4	466.891	1.373

3 CONCLUSION

This paper investigates the impact of laser process parameters on the surface texture characteristics of POM. The predictive model was established to correlate three laser parameters (laser power, scanning speed, and pulse width) with texture depth and surface roughness at the bottom of the texture. The grey-Taguchi method was employed for multi-objective optimization and experimental verification of the process parameters. The results indicate that with the increase of laser power and the decrease of scanning speed, the depth of the weave gradually increases, but its increase decreases with the further change of these two influencing factors. The surface roughness at the bottom of the texture decreases with increasing pulse width and exhibits a trend of initially increasing and then decreasing with increasing scanning speed, with a maximum value observed at a power of 24 W. The variation of pulse width has no significant effect on either the depth or surface roughness. Multi-objective optimization using the grey-Taguchi method resulted in obtaining the optimal combination of laser parameters as $A_5B_1C_1$ (laser power is 30 W, the scanning speed is 400 mm/s and pulse width is 4 μs). Compared with the corresponding data obtained from the orthogonal experiments, the texture depth increased by 3.42 %, and the surface roughness of the bottom surface decreased by 10.08 % under the optimal parameter combination, achieving a significant optimization of surface roughness while obtaining a larger depth. Experimental validation of the established prediction model using the optimal parameter combination showed that the predicted values of depth and surface roughness had errors of 1.86 % and 7.60 %, respectively, compared to the experimental measurements, and the model was accurate enough to achieve accurate prediction of the surface texture properties of POM.

4 ACKNOWLEDGEMENTS

Financial support for this work was provided by the National Natural Science Foundation of China Youth Project (Grant no. 51905170) and the Natural Science Foundation of Hunan Province (Grant no. 2020JJ4334).

5 REFERENCES

[1] Siddiqui, M.N.S., Pogacnik, A., Kalin, M. (2022). Influence of load, sliding speed and heat-sink volume on the tribological behaviour of polyoxymethylene (POM) sliding against steel. *Tribology International*, vol. 178, part A, art. ID 108029, **DOI:10.1016/j.triboint.2022.108029**.

[2] Friedrich, K. (2018). Polymer composites for tribological applications. *Advanced Industrial and Engineering Polymer Research*, vol. 1, no. 1, p. 3-39, **DOI:10.1016/j.aiepr.2018.05.001**.

[3] Li, J.H., Wang, Y.T., Wang, X.D., Wu, D.Z. (2019). Crystalline characteristics, mechanical properties, thermal degradation kinetics and hydration behavior of biodegradable fibers melt-spun from Polyoxymethylene/Poly(L-lactic acid) blends. *Polymers*, vol. 11, no. 11, art. ID 1753, **DOI:10.3390/polym11111753**.

[4] Matkovič, S., Kalin, M. (2021). Effects of slide-to-roll ratio and temperature on the tribological behaviour in polymer-steel contacts and a comparison with the performance of real-scale gears. *Wear*, vol. 477, art. ID 203789, **DOI:10.1016/j.wear.2021.203789**.

[5] Bazan, P., Kuciel, S., Nykiel, M. (2019). Characterization of composites based on polyoxymethylene and effect of silicone addition on mechanical and tribological behavior. *Polymer Engineering & Science*, vol. 59, no. 5, p. 935-940, **DOI:10.1002/pen.25039**.

[6] Guo, X., Zhang, J., Huang, J. (2015). Poly(lactic acid)/polyoxymethylene blends: Morphology, crystallization, rheology, and thermal mechanical properties. *Polymer*, vol. 69, p. 103-109, **DOI:10.1016/j.polymer.2015.05.050**.

[7] Zhou, Z.Z., Chu, Y.H., Hou, Z.S., Zhou, X.P., Cao, Y. (2022). Modification of frictional properties of hydrogel surface via laser ablated topographical micro-textures. *Nanomaterials*, vol. 12, no. 22, art. ID 4103, **DOI:10.3390/nano12224103**.

[8] Xiao, J.R., Zhang, Y.T., Hu, B., Liu, X.C., Liang, Z.W., Zhao, Z. (2023). Tribological properties of Ti6Al4V alloy composite texture fabricated by ultrasonic strengthening grinding and laser processing. *Materials*, vol. 16, no. 1, art. ID 355, **DOI:10.3390/ma16010355**.

[9] Lu, L.B., Zhang, Z., Guan, Y.C., Zheng, H.Y. (2018). Comparison of the effect of typical patterns on friction and wear properties of chromium alloy prepared by laser surface texturing. *Optics & Laser Technology*, vol. 106, p. 272-279, **DOI:10.1016/j.optlastec.2018.04.020**.

[10] Hoskins, J.K., Zou, M. (2021). Designing a bioinspired surface for improved wear resistance and friction reduction. *Journal of Tribology*, vol. 143, no. 5, art. ID 051107, **DOI:10.1115/1.4050673**.

[11] Xu, S., An, S.O.J., Atsushi, D., Castagne, S. (2016). Development of low-cost deformation-based micro surface texturing system for friction reduction. *International Journal of Precision Engineering and Manufacturing*, vol. 17, p. 1059-1065, **DOI:10.1007/s12541-016-0128-3**.

[12] Li, W.W., Xue, W.B. (2023). Structural characterization of AlN thin films grown on sapphire by atomic layer deposition. *Thin Solid Films*, vol. 773, art. ID 139826, **DOI:10.1016/j.tsf.2023.139826**.

[13] Costa, H., Hutchings, I. (2014). Some innovative surface texturing techniques for tribological purposes. *Proceedings of the Institution of Mechanical Engineers, Part J: Journal of Engineering Tribology*, vol. 229, no. 4, p. 429-448, **DOI:10.1177/1350650114539936**.

[14] Su, X., Shi, L.P., Huang, W., Wang, X.L. (2016). A multi-phase micro-abrasive jet machining technique for the surface texturing of mechanical seals. *The International Journal of Advanced Manufacturing Technology*, vol. 86, p. 2047-2054, **DOI:10.1007/s00170-015-8272-y**.

[15] Stratakis, E., Bonse, J., Heitz, J., Tsibidis, G.D., Skoulas, E., Papadopoulos, A., Mimidis, A., Joel, A.-C., Comanns, P., Krüger, J., Florian, C., Fuentes-Edfuf, Y., Solis, J., Baumgartner, W. (2020). Laser engineering of biomimetic surfaces. *Materials Science and Engineering R: Reports*, vol. 141, art. ID 100562, **DOI:10.1016/j.mser.2020.100562**.

[16] Liu, Y., Li, X., Jin, J., Liu, J., Yan, Y., Han, Z., Ren, L. (2017). Anti-icing property of bio-inspired micro-structure superhydrophobic surfaces and heat transfer model. *Applied Surface Science*, vol. 400, p. 498-505, **DOI:10.1016/j.apsusc.2016.12.219**.

[17] Cho, M.H., Park, S. (2011). Micro CNC surface texturing on polyoxymethylene (POM) and its tribological performance in lubricated sliding. *Tribology International*, vol. 44, no. 7-8, p. 859-867, **DOI:10.1016/j.triboint.2011.03.001**.

[18] Cheng, H., Zhou, F., Fei, Z.H. (2023). Dry friction properties of friction subsets and angle related to surface texture of cemented carbide by femtosecond laser surface texturing. *Coatings*, vol. 13, no. 4, art. ID 741, **DOI:10.3390/coatings13040741**.

[19] Alnusirat, W., Kyrychok, M., Bellucci, S., Gnilitskyi, I. (2021). Impact of ultrashort laser nanostructuring on friction properties of AISI 314 LVC. *Symmetry*, vol. 13, no. 6, art. ID 1049, **DOI:10.3390/sym13061049**.

[20] Liu, Y.Y., Liu, L.L., Deng, J.X., Meng, R., Zou, X.Q., Wu, F.F. (2017). Fabrication of micro-scale textured grooves on green ZrO2 ceramics by pulsed laser ablation. *Ceramics International*, vol. 43, p. 6519-6531, **DOI:10.1016/j.ceramint.2017.02.074**.

[21] Li, D.X., Chen, X.X., Guo, C.H., Tao, J., Tian, C.X., Deng, Y.M., Zhang, W.W. (2017). Micro surface texturing of alumina ceramic with nanosecond laser. *Procedia Engineering*, vol. 174, p. 370-376, **DOI:10.1016/j.proeng.2017.01.155**.

[22] Cheng, B.X., Duan, H.T., Chen, Q., Shang, H.F., Zhang, Y., Li, J., Shao, T.M. (2021). Effect of laser treatment on the tribological performance of polyetheretherketone (PEEK) under seawater lubrication. *Applied Surface Science*, vol. 566, art. ID 150668, **DOI:10.1016/j.apsusc.2021.150668**.

[23] Zhao, W.Q., Shen, X.W., Liu, H.D., Wang, L.Z., Jiang, H.T. (2020). Effect of high repetition rate on dimension and morphology of micro-hole drilled in metals by picosecond ultra-short pulse laser. *Optics and Lasers in Engineering*, vol. 124, art. ID 105811, **DOI:10.1016/j.optlaseng.2019.105811**.

[24] Deepu, P., Jagadesh, T., Muthukannan, D., Jagadeesh, B. (2023). Investigation into femtosecond based laser ablation and morphology of micro-hole in titanium alloy. *Optik*, vol. 274, art. ID. 170519, **DOI:10.1016/j.ijleo.2023.170519**.

[25] Lian, G.F., Yao, M.P., Zhang, Y., Chen, C.R. (2018). Analysis and prediction on geometric characteristics of multi-track overlapping laser cladding. *The International Journal of Advanced Manufacturing Technology*, vol. 97, p. 2397-2407, **DOI:10.1007/s00170-018-2107-6**.

[26] Cui, L.J., Zhang, M., Guo, S.R., Cao, Y.L., Zeng, W.H., Li, X.L., Zheng, B. (2020). Multi-objective numerical simulation of geometrical characteristics of laser cladding of cobalt-based alloy based on response surface methodology. *Measurement and Control*, vol. 54, no. 7-8, p. 1125-1135, **DOI:10.1177/0020294020944955**.

[27] Ren, Y.M., Zhang, Z.Y. (2022). Surface of nanosecond laser polished single-crystal silicon improved by two-step laser irradiation. *Acta Optica Sinica*, vol. 42, no. 7, p. 212-219, **DOI:10.3788/AOS202242.0714004**. (in Chinese)

[28] Suthar, J., Teli, S.N., Murumkar, A. (2021). Drilling process improvement by Taguchi method. *Materials Today: Proceedings*, vol. 47, p. 2814-2819, **DOI:10.1016/j.matpr.2021.03.533**.

[29] Deng, D.W., Li, T.S., Huang, Z.Y., Jiang. H., Yang, S.H., Zhang, Y. (2022). Multi-response optimization of laser cladding for TiC particle reinforced Fe matrix composite based on Taguchi method and grey relational analysis. *Optics & Laser Technology*, vol. 153, art. ID 108259, **DOI:10.1016/j.optlastec.2022.108259**.

[30] Volpe, V., Speranza, V., Schrank, T., Berer, M., Pantani, R. (2022). An investigation of crystallization kinetics of polyoxymethylene in processing conditions. *Polymers for Advanced Technologies*, vol. 34, no. 2, p. 634-645, **DOI:10.1002/pat.5916**.

[31] Chen, W.H., Uribe, M.C., Kwon, E.E, Lin, K.Y.A., Park, Y.K., Ding., L, Saw Huat, L. (2022). A comprehensive review of thermoelectric generation optimization by statistical approach: Taguchi method, analysis of variance (ANOVA), and response surface methodology (RSM). *Renewable and Sustainable Energy Reviews*, vol. 169, art. ID 112917, **DOI:10.1016/j.rser.2022.112917**.